J Mater Sci: Mater Electron (2014) 25:4512–4516
DOI 10.1007/s10854-014-2197-3

Fabrication and optical properties of ZnS:Mn^{2+} quantum dots/SiO_2 nanocomposites

Jian Cao · Tingting Wang · Jinghai Yang · Xiaofu Zhou · Donglai Han · Shuo Yang · Qianyu Liu · Haifeng Niu

Received: 19 May 2014 / Accepted: 19 July 2014 / Published online: 29 July 2014

Abstract ZnS:Mn^{2+} quantum dots (QDs)/SiO_2 nanocomposites were successfully synthesized by stöber method. The results showed that the Mn^{2+} ions were substitutionally incorporated into the ZnS host and the average size of the ZnS:Mn^{2+} (5 %) QDs was about 5.5 nm. The yellow–orange emission from the Mn^{2+} $^4T_1$–$^6A_1$ transition was observed in the photoluminescence spectra, the peak intensity increased as the Mn^{2+} doped ratio increased, and showed a maximum when the concentration of the Mn^{2+} ions kept at 3 %. As the hydrolysis time of tetraethyl orthosilicate increased, the intensity of the yellow–orange emission reached the highest value when $t = 4$ h for the ZnS:Mn^{2+} (5 %) QDs/SiO_2 nanocomposites.

J. Cao (✉) · T. Wang · J. Yang (✉) · Q. Liu · H. Niu
Key Laboratory of Functional Materials Physics and Chemistry of the Ministry of Education, Jilin Normal University, Siping 136000, People's Republic of China
e-mail: caojian_928@163.com

J. Yang
e-mail: jhyang1@jlnu.edu.cn

T. Wang · X. Zhou
Key Laboratory of Plant Resources Science and Green Production of Jilin Province, Jilin Normal University, Siping 136000, People's Republic of China

D. Han · S. Yang
Changchun Institute of Optics, Fine Mechanics and Physics, Chinese Academy of Sciences, Changchun 130033, People's Republic of China

1 Introduction

In the past decades, the monodispersed fluorescent semiconductor nanoparticles quantum dots (QDs) have attracted much more attention in comparison with organic dyes especially in bio-imaging fields due to their unique optical and electronic properties, such as remarkable quantum yield (quantum yield ~60–70 %), size tunable photoluminescence, broad excitation with narrow emission bands, excellent photostability and highly photobleaching resistance etc. [1–4]. Among the widely studied II–VI semiconductor nanomaterials, ZnS has great advantages as follows: (1) low toxicity, (2) high photostability, (3) relative lower price, (4) simple synthesis procedure [5]. It is well known that doping Mn^{2+} ions into the ZnS lattice can give rise to the strong yellow–orange light emission located at about 583 nm (through the $^4T_1$ to $^6A_1$ internal transition) with a high quantum yield, the luminescence lifetime of which is about 1 ms [6]. Such a strong luminescence and long lifetime can make the light penetrate into and out of the tissues and distinguish the luminescence from the background autofluorescence. These excellent optical properties make the ZnS:Mn^{2+} nanocrystals to be the potential candidates as the fluorescent labeling agents.

To improve the reliability and stability of the ZnS:Mn^{2+} QDs, the silica coating has been proved to be an ideal protection method for nanocrystals because of the excellent chemical stability, biocompatibility and easily furthered conjugation with various functional groups [7]. In principle, ZnS:Mn^{2+} QDs/SiO_2 would exhibit good photostability and high luminescent efficiency.

In this paper, we present the fabrication of the monodispersed ZnS:Mn^{2+} QDs and ZnS:Mn^{2+} QDs/SiO_2 nanocomposites. We not only provide the simple preparation method but also investigate the photoluminescent (PL)

properties of the ZnS:Mn^{2+} QDs and ZnS:Mn^{2+} QDs/SiO_2 nanocomposites.

2 Experimental section

2.1 Materials

Zinc acetate, manganese acetate, sodium sulfide, oleic acid, sodium oleate, ammonium bicarbonate, cetyltrimethylammonium bromide (CTAB), tetraethyl orthosilicate (TEOS), cyclohexane and ethanol (98 %) are all analytical grade (Shanghai Chemical Reagents Co.) and used without further purification.

2.2 Synthesis of ZnS:Mn^{2+} QDs

Oleic acid stabilized $Zn_{1-x}Mn_xS$ (x = 0.01, 0.03, 0.05, 0.07, 0.10) QDs were synthesized according to the reported method [8]. In a typical process, 6 mmol of zinc acetate and x mmol of manganese acetate (x = 0.06, 0.18, 0.30, 0.42, 0.60) were dissolved in 7 ml of deionized water to form a transparent solution (solution A). Then, 6 mmol of sodium sulfide were dissolved in 7 ml deionized water to form a transparent solution (solution B). After stirring for 10 min, 9.75 ml of oleic acid, 1.3 g of sodium oleate and 16 ml of ethanol were put into solution A. After stirring for 1 h, solution B was added to solution A. After stirring for 2 h, the colloid solution was transferred into a 50 ml Teflon-lined autoclave and kept at 190 °C for 12 h. After the reaction, the autoclave was taken out and cooled down to room temperature. The product was washed with ethanol/cyclohexane mixture for several times and separated by centrifugation, and then dried at 80 °C for 2 h.

2.3 Synthesis of ZnS:Mn^{2+} QDs/SiO_2 nanocomposites

The ZnS:Mn^{2+} QDs/SiO_2 nanocomposites were synthesized by stöber method. In a typical process, 50 ml of absolute alcohol, 1 ml of distilled water, 1.7 ml of aqueous ammonia, and 200 μl of TEOS were injected into a 100 ml conical flask; this solution was stirred for 10 min at room temperature. After that, ZnS:Mn^{2+} (5 %) QDs (0.008 g) and CTAB (0.1 g) dispersed ultrasonically in distilled water (10 ml) were added to the foregoing solution. To investigate the effect of the SiO_2 thickness on the optical properties of the samples, the mixture was continuously stirred for 2, 4, 6 h at room temperature, respectively. The resulting nanocomposites were then isolated by centrifugation and washed with the hot deionized water to remove excess QDs as well as CTAB as much as possible, which could avoid the adverse effects of CTAB on the surface property of the product. For each washing, the sonicator was used to completely disperse the nanoparticles in water and drying in an oven for 4 h at 50 °C.

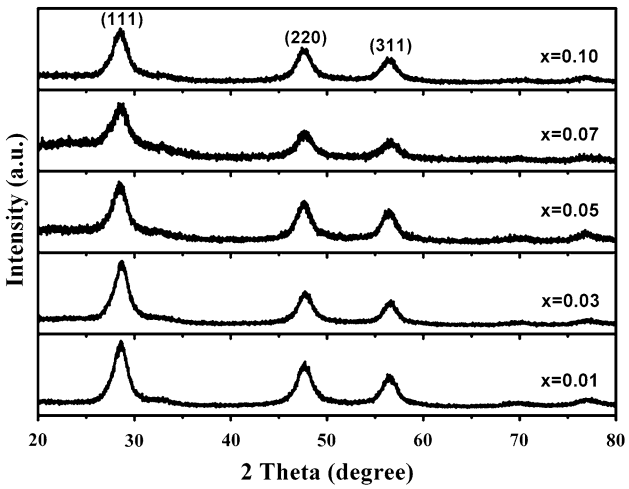

Fig. 1 XRD patterns of the $Zn_{1-x}Mn_xS$ (x = 0.01, 0.03, 0.05, 0.07, 0.10) QDs

2.4 Characterization of products

X-ray diffraction (XRD) pattern was collected on a MAC Science MXP-18 X-ray diffractometer using a Cu target radiation source. Transmission electron micrographs (TEM) and high-resolution transmission electron microscopy (HRTEM) images were taken on JEM-2100 electron microscope. The specimen was prepared by depositing a drop of the dilute solution of the sample in ethanol on a carbon-coated copper grid and drying at room temperature. UV–Vis absorption spectrum was measured on UV-3101PC UV spectrometer. The specimen for the measurement was dispersed in ethanol and placed in a 1 cm quartz cell, and ethanol served as the reference. Photoluminescence (PL) measurement was carried out at room temperature, using 325 nm as the excitation wavelength, He–Cd Laser as the source of excitation.

3 Results and discussion

Figure 1 displays the XRD patterns of the $Zn_{1-x}Mn_xS$ (x = 0.01, 0.03, 0.05, 0.07, 0.10) QDs. For the $Zn_{0.99}Mn_{0.01}S$ QDs, three main peaks at 28.58° (111), 47.65° (220) and 56.49° (311) can be observed, which are in good agreement with the standard card (JCPDS No. 05-0566). According to the Bragg's equation [9], the lattice constant of the $Zn_{0.99}Mn_{0.01}S$ QDs is calculated to be 5.3971 Å (x = 0.01), and a slight increase is obtained in the lattice constant of the $Zn_{1-x}Mn_xS$ QDs as the Mn^{2+} doped ratio

Table 1 Lattice constant and particle size of the $Zn_{1-x}Mn_xS$ (x = 0.01, 0.03, 0.05, 0.07, 0.10) QDs calculated from XRD

Sample	Lattice constant (Å)	Particle size (nm)
$Zn_{0.99}Mn_{0.01}S$	$a = 5.3971$	5.51
$Zn_{0.97}Mn_{0.03}S$	$a = 5.3995$	5.32
$Zn_{0.95}Mn_{0.05}S$	$a = 5.4097$	5.20
$Zn_{0.93}Mn_{0.07}S$	$a = 5.4097$	5.11
$Zn_{0.90}Mn_{0.10}S$	$a = 5.4099$	5.07

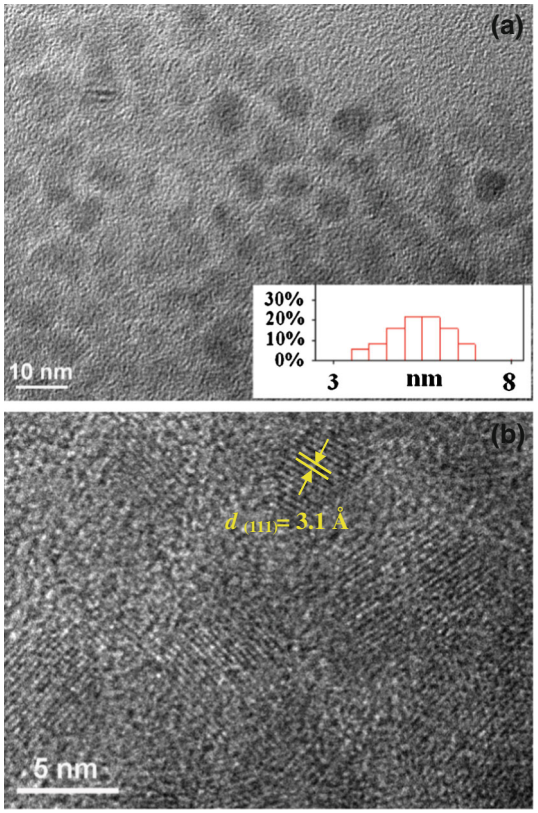

Fig. 2 **a**, **b** TEM and HRTEM images of the $Zn_{0.95}Mn_{0.05}S$ QDs

increased, which can be seen in Table 1. Since that the ionic radius of the Mn^{2+} ions (0.83 Å) is 10 % larger than that of the Zn^{2+} ions (0.74 Å), the lattice expansion can be observed if the Mn^{2+} ions substituted for the Zn^{2+} sites. In addition, there is no extra diffraction peak from the manganese ions, which indicates that the Mn^{2+} ions may be incorporated into the ZnS lattice. The average size estimated from the full width at half-maximum of the three main peaks using Debye–Scherrer formula [10] is about 5.51 nm (x = 0.01), 5.32 nm (x = 0.03), 5.20 nm (x = 0.05), 5.11 nm (x = 0.07) and 5.07 nm (x = 0.07; Table 1). So, the particle size is decreased as the Mn^{2+} doped ratio increased.

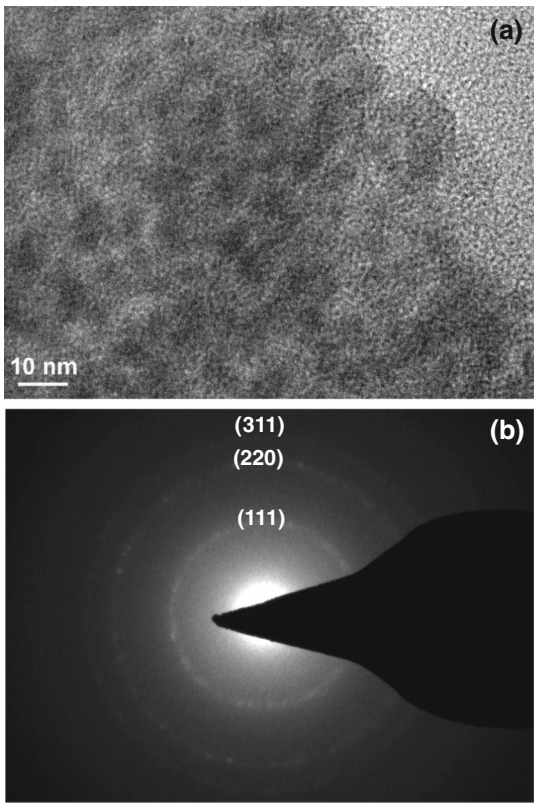

Fig. 3 TEM and SAED images of the $Zn_{0.95}Mn_{0.05}S$ QDs/SiO_2 nanocomposites when t = 4 h

Figure 2 shows the TEM and HRTEM images of the synthesized $Zn_{0.95}Mn_{0.05}S$ QDs. These QDs are uniform and monodispersed, with the average diameter of about 5.5 nm, which is consistent with the value calculated from XRD. The HRTEM image (Fig. 2b) exhibits a clear lattice spacing of 3.1 Å, which matches with the distance of the (111) plane of the cubic ZnS [11].

Figure 3 displays the TEM and selected area electron diffraction (SAED) images of the $Zn_{0.95}Mn_{0.05}S$ QDs/SiO_2 nanocomposites when t = 4 h. As can be seen from the TEM image (Fig. 3a), the surface is not smooth, which indicates that the $Zn_{0.95}Mn_{0.05}S$ QDs are successfully embedded within the SiO_2 matrix. These QDs are well crystallized, which are consistent with that of the QDs in Fig. 2a. Considering our XRD study and close observation of the SAED image (Fig. 3b), it can be concluded that the diffraction rings represent the cubic structure of ZnS.

Figure 4 shows the UV–Vis spectra of the $Zn_{1-x}Mn_xS$ QDs. The absorption maxima for the $Zn_{1-x}Mn_xS$ (x = 0.01, 0.03, 0.10) QDs is 321.06 nm (x = 0.01), 319.26 nm (x = 0.03) and 318.82 nm (x = 0.10), respectively, which is blue shift as the Mn doped ratio increased. It is well known that ZnS is a direct gap semiconductor. The optical band gap 'Eg' can be calculated using the following relation:

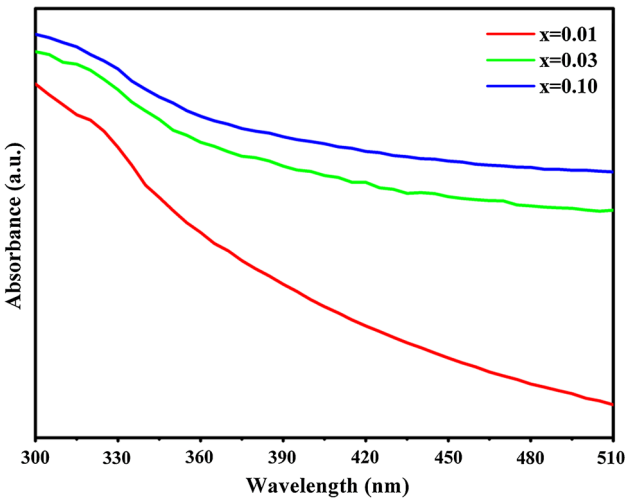

Fig. 4 UV–Vis absorption spectra of the $Zn_{1-x}Mn_xS$ (x = 0.01, 0.03, 0.10) QDs

$$\alpha = A(hv - Eg)^n/hv.$$

where A is a constant and n is a constant, equal to 1/2 for the direct band gap semiconductor. We found that the band gap of the $Zn_{1-x}Mn_xS$ (x = 0.01, 0.03, 0.10) QDs is 3.86 eV (x = 0.01), 3.88 eV (x = 0.03) and 3.89 eV (x = 0.10), respectively, which indicates that the size of the particles is decreased as the Mn doped ratio increased.

Figure 5 presents the PL spectra of the $Zn_{1-x}Mn_xS$ (x = 0.01, 0.03, 0.05, 0.10) QDs and $Zn_{0.95}Mn_{0.05}S$ QDs/SiO_2 nanocomposites. For all the samples in Fig. 5a, the blue–green emission ranging from 400 to 520 nm can be ascribed to the defect states in the ZnS QDs (S vacancy, Zn vacancy and surface states [12–15]), the yellow–orange emission centered at ~588 nm is associated with the $^4T_1$–$^6A_1$ transition within the 3*d* shell of the Mn^{2+} ions. According to Bhargava et al. [16], the yellow–orange emission is attributed to the efficient energy transfer from the ZnS host to the Mn^{2+} ions facilitated by the mixed electronic states. When the Mn^{2+} ions are incorporated into the ZnS lattice and substitute for the cation sites, the mixing between the *s*–*p* electrons of the host ZnS and the *d* electrons of the Mn^{2+} ions occurs and makes the forbidden transition of $^4T_1$–$^6A_1$ partially allowed, resulting in the characteristic emission of the Mn^{2+} ions. Previously, Sooklal et al. [17] studied the effect of the location of Mn^{2+} on the photophysics of ZnS nanoparticles. They found that Mn^{2+} incorporation into the ZnS lattice has led to the orange emission while ZnS with surface-bound Mn^{2+} yielded the ultraviolet emission. As a comparison with our own results, it can be suggested that the Mn^{2+} ions are incorporated into the ZnS QDs. As the Mn^{2+} ions doped ratio increased, the peak intensity of the

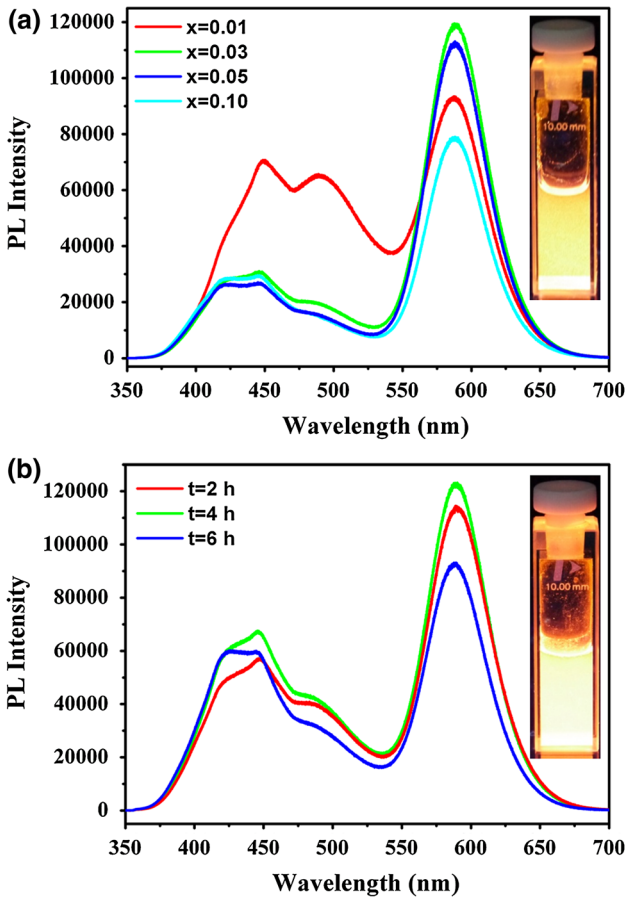

Fig. 5 **a** PL spectra of the $Zn_{1-x}Mn_xS$ (x = 0.01, 0.03, 0.05, 0.10) QDs; **b** PL spectra of the $Zn_{0.95}Mn_{0.05}S$ QDs/SiO_2 nanocomposites when t = 2, 4, 6 h; the *inset* images in **a**, **b** is the photographic images of the water solution of the ZnS:Mn^{2+} QDs and ZnS:Mn^{2+} QDs/SiO_2 nanocomposites under UV illumination (λ = 365 nm)

yellow–orange emission keep increasing until the concentration of the Mn^{2+} ions is up to 3 % and then slightly decrease when the concentration of the Mn^{2+} ions continually increase to 10 %. As the Mn^{2+} doped ratio increased, the concentration quenching effect can be observed. It maybe due to that the inhomogeneous distribution of the Mn^{2+} ions, local Mn^{2+}–Mn^{2+} pairs or clusters were formed in the ZnS crystals, which interacted each with other and led to the nonradiative relaxation under excitation [18].

Figure 5b show the PL spectra of the $Zn_{0.95}Mn_{0.05}S$ QDs/SiO_2 nanocomposites when t = 2, 4, 6 h. For the yellow–orange emission, the luminescent intensity keeps increasing until t = 4 h and then decreases gradually when the time continually increase to 6 h. In fact, the intensity of the emission is mainly determined by the degree of surface passivation. At the early stage of the hydrolysis of TEOS, only parts of ZnS:Mn^{2+} QDs were encapsulated by the silica shell, while the rest of QDs still remained in the

solution, which can be removed in the experiment. So, the surface of ZnS:Mn^{2+} QDs can be passivated fully by SiO_2. With the increase in the hydrolysis time of TEOS, the silica shell became thick and more ZnS:Mn^{2+} QDs would be encapsulated. But the thick SiO_2 coating would induce strain at the interface caused by the lattice mismatch between each other. It would result in new traps for carriers, which are thought to be the main reason for the decrease in the yellow–orange [19]. The photographic images in the inset image of Fig. 5a, b shows that the water solution of the as-synthesized nanocomposites is orange and the brightness is increased after the SiO_2 passivation.

4 Conclusion

In this paper, we have synthesized the ZnS:Mn^{2+} QDs/SiO_2 nanocomposites. The PL intensity of the yellow–orange emission can be observed and tuned by regulating the concentration of the Mn^{2+} ions and the hydrolysis time of TEOS. The results showed that the luminescence intensity of the yellow–orange emission reached the highest value when t = 4 h for the $Zn_{0.95}Mn_{0.05}S$ QDs/SiO_2.

Acknowledgments This work was financially supported by the National Programs for High Technology Research and Development of China (863) (Item No. 2013AA032202), the National Natural Science Foundation of China (Grant Nos. 61008051, 61178074, 11204104, 11254001, 61378085, 61308095).

References

1. M. Bruchez, M. Moronne, P. Gin, S. Weiss, A. Alivisatos, Science **281**, 2013 (1998)
2. S. Coe, W.K. Woo, M. Bawendi, V. Bulovic, Nature **420**, 800 (2002)
3. I.L. Medintz, H.T. Uyeda, E.R. Goldman, H. Mattoussi, Nat. Mater. **4**, 435 (2005)
4. X. Michalet, F.F. Pinaud, L.A. Bentolila, J.M. Tsay, S. Doose, J.J. Li, G. Sundaresan, A.M. Wu, S.S. Gambhir, S. Weiss, Science **307**, 538 (2005)
5. X. Yu, J. Wan, Y. Shan, K. Chen, X. Han, Chem. Mater. **21**, 4892 (2009)
6. L. Liu, L. Xiao, H. Zhu, Chem. Phys. Lett. **539**, 112 (2012)
7. H.L. Ding, Y.X. Zhang, S. Wang, J.M. Xu, S.C. Xu, G.H. Li, Chem. Mater. **24**, 4572 (2012)
8. X. Wang, J. Zhuang, Q. Peng, Y.D. Li, Nature **437**, 21 (2005)
9. Z.W. Quan, Z.L. Wang, P.P. Yang, J. Lin, J.Y. Fang, Inorg. Chem. **46**, 1354 (2007)
10. P.V.B. Lakshmi, K.S. Raj, K. Ramachandran, Cryst. Res. Technol. **44**, 153 (2009)
11. W.Q. Peng, S.C. Qu, G.W. Cong, Z.G. Wang, J. Cryst. Growth **282**, 179 (2005)
12. M.V. Limaye, S. Gokhale, S.A. Acharya, S.K. Kulkarni, Nanotechnology **19**, 415602 (2008)
13. P. Hu, Y. Liu, L. Fu, L. Cao, D. Zhu, J. Phys. Chem. B **108**, 936 (2004)
14. N. Pradhan, S. Efrima, J. Phys. Chem. B **108**, 11964 (2004)
15. Z. Li, B. Liu, X. Li, S. Yu, L. Wang, Y. Hou, Y. Zou, M. Yao, Q. Li, B. Zou, T. Cui, G. Zou, G. Wang, Y. Liu, Nanotechnology **18**, 255602 (2007)
16. R.N. Bhargava, D. Gallagher, Phys. Rev. Lett. **72**, 416 (1994)
17. K. Sooklal, B.S. Cullum, S.M. Angel, C.J. Murphy, J. Phys. Chem. **100**, 4551 (1996)
18. I. Yu, M. Senna, Appl. Phys. Lett. **66**, 23 (1995)
19. J. Cao, J.H. Yang, L.L. Yang, M.B. Wei, B. Feng, D.L. Han, L. Fan, B.J. Wang, H. Fu, J. Appl. Phys. **112**, 014316 (2012)